Cement & Concrete Composites 53 (2014) 187–199

Contents lists available at ScienceDirect

Cement & Concrete Composites

journal homepage: www.elsevier.com/locate/cemconcomp

Post-fire mechanical performance of concrete made with selected plastic waste aggregates

J.R. Correia *, J.S. Lima, J. de Brito

Department of Civil Engineering and Architecture, Instituto Superior Técnico/ICIST, Universidade de Lisboa. Av. Rovisco Pais 1, 1049-001 Lisbon, Portugal

ARTICLE INFO

Article history:
Received 1 November 2013
Received in revised form 8 June 2014
Accepted 6 July 2014
Available online 16 July 2014

Keywords:
Recycled plastic waste aggregates
PET
Elevated temperature
Residual performance
Mechanical properties
Post-fire assessment

ABSTRACT

This paper presents an experimental study about the effects of elevated temperatures on the residual mechanical properties of concrete incorporating selected plastic waste aggregates (PWAs). Six different concrete mixes were prepared: a reference concrete (RC) made with natural aggregates (NAs) and five concrete mixes with replacement ratios of 7.5% and 15% of natural aggregate by three types of polyethylene terephthalate (PET) plastic waste aggregate (CPWA). Specimens were exposed to temperatures of 600 °C and 800 °C for a period of 1 h, after being heated in accordance with the ISO 834 time–temperature curve. After cooling down to ambient temperature, the following properties were evaluated and compared with reference values obtained prior to fire exposure: (i) compressive and (ii) splitting tensile strengths, (iii) elastic modulus, (iv) ultrasonic pulse velocity (UPV), (v) surface hardness, and (vi) water absorption by immersion. For the replacement ratios used in these experiments, the maximum temperatures reached in CPWA were higher than those measured in RC, due to the higher porosity increase with temperature of the former type of concrete that facilitated the propagation of heat inside concrete, and the exothermic thermal decomposition of plastic aggregates that generated additional heat. After exposure to elevated temperatures, the degradation of compressive strength and elastic modulus of CPWA was higher than that of RC, particularly for the highest replacement ratio, as a consequence of the higher porosity increase experienced by CPWA. The reduction of residual splitting tensile strength of CPWA was found to be similar to that of RC, possibly because the incorporation of PWA led to lower internal stresses due to thermal gradients and allowed an easier dispersion of gases confined in pores, thus reducing crack development in the matrix. The magnitude of the degradation of concrete's residual mechanical properties was seen to depend on the type of PWAs and the replacement ratio. The residual compressive strength of CPWA proved to be strongly correlated with both UPV and water absorption by immersion, but its correlation with surface hardness was less significant.

1. Introduction

Modern plastics proved to be one of the most revolutionary materials developed in the twentieth century, with numerous applications in several industries, such as packaging, building and construction, automotive, electrical and electronics. Since their development in the 1930s, the consumption of plastics has been increasing consistently and considerably. Between 1950 and 2011, the annual world production of plastics increased from 1.7 to 280 million tons [1]. Among the several types of plastics produced, polyethylene terephthalate (PET) is one of the most relevant, presently corresponding to about 7% of the above mentioned figures [1].

A considerable proportion of products and goods made of plastics are generally discarded soon after being produced (e.g., PET water and soda bottles, food packages), generating huge amounts of plastic post-consumer waste. The production of this type of waste will continue to increase in the future. In fact, it has been estimated that the annual production of plastic waste doubles every 10 years [2].

Presently, the management of plastic waste is far from being sustainable. According to a study carried out at Columbia University by Themelis et al. [3], in the United States of America, in 2008, 85.8% of plastic waste was landfilled, 7.7% was incinerated, while only 6.5% was recycled. According to the European Association of Plastics Manufacturers, a better (and improving) plastic waste management practice has been followed in Europe, resulting in the following statistics (average between 2006 and 2011): 51% (landfill), 27% (incineration) and 22% (recycling) [1]. Overall, these

* Corresponding author. Tel.: +351 218 418 212; fax: +351 218 488 481.
E-mail address: jcorreia@civil.ist.utl.pt (J.R. Correia).

http://dx.doi.org/10.1016/j.cemconcomp.2014.07.004
0958-9465/

figures draw attention to the need to increase the levels of plastic waste recycling, namely taking into account (i) the limited availability of landfills and increasingly stringent legislation, (ii) the environmental risks in terms of soil contamination (caused by the chemical aggressiveness of this type of waste) and fire deflagration (due to their combustible nature), and (iii) the intrinsic resistance of this type of waste to atmospheric and biological agents [4].

Although there are several recycling possibilities, the reuse of solid plastic waste to produce other materials, namely concrete, stands out as one of the most economical and sustainable alternatives to dispose of this type of waste [5]. Several studies have addressed the technical viability of incorporating selected plastic waste in concrete, investigating the effects of such incorporation on the mechanical and durability properties of concrete.

The literature [5–10] on the mechanical performance of concrete made with plastic waste aggregates (CPWA), with emphasis on PET aggregates, seems to be relatively consensual. As a matter of fact, even small incorporation ratios not exceeding 15% of the natural aggregates volume can cut by half the most important mechanical properties of concrete (compressive and tensile strength, and elastic modulus) made with plastic aggregates by comparison with a reference concrete with natural aggregates only.

As for the durability behaviour of CPWA, the literature is less abundant [7,11–13]. Its results are also less consensual, namely in terms of shrinkage and carbonation and chloride penetration (opposite trends have been found by comparison with a reference concrete), while there is consensus that the water absorption, both by capillarity and immersion, increases as the ratio of replacement of natural aggregates by recycled plastic aggregates increases.

The above mentioned studies provide a reasonable understanding about the mechanical and durability performance of CPWA, showing that their mechanical performance decreases monotonically with the replacement ratio, but some of the durability-related properties may be improved with the incorporation of these aggregates. However, in order to enable the widespread use of this material in civil engineering applications, namely in buildings, it is also important to assess the fire behaviour of CPWA, particularly if taking into account the legitimate concerns raised by the combustible nature of this type of recycled material.

The main goal of this study is to investigate the behaviour of CPWA when subjected to high temperatures, in terms of thermal response and residual mechanical properties. For this purpose, six types of concrete mixes were produced: a reference concrete (RC) and five concrete mixes incorporating 7.5% or 15% of three different types of PET plastic waste aggregates (PWAs) as a replacement of natural aggregates (NAs). All concrete mixes were exposed, for 1 h, to furnace temperatures of 600 °C and 800 °C, after being heated according to the nominal curve defined in ISO 834 [14]. It is worth mentioning that the main goal of the experiments was not to perform a full and thorough characterization of the post-fire residual mechanical performance of CPWA, but rather to assess the direct influence of incorporating PWA on such performance.

2. Literature review and research significance

Numerous studies were conducted in the past on the fire behaviour of normal strength conventional concrete. Those studies have provided a comprehensive understanding of the main physical–chemical deterioration mechanisms underwent by concrete and its main components at different temperatures [15–17]. In addition, they allowed establishing reference curves that define the variation of the main physical and mechanical properties of concrete as a function of the temperature, both in hot and in residual conditions (e.g., [18,19]).

More recently, the fire behaviour of different types of concrete has also been the object of research. Among the types of concrete whose fire behaviour is relatively well documented in the literature are high strength concrete (e.g., [20,21]), fibre reinforced concrete (e.g., [22,23]), lightweight concrete (e.g., [24,25]), aerated concrete [26] and concrete containing different types of supplementary cementing materials, such as blast furnace slag (e.g., [27,28]), fly ash (e.g., [29,30]) or silica fume (e.g., [31,32]).

In the past few years, exploratory studies were also performed on the fire behaviour of concrete incorporating different types of recycled aggregates. Those studies, recently reviewed by Cree et al. [33], focus on the effects of incorporating different types of recycled aggregate, namely ceramic material (e.g., [34,35]), concrete (e.g., [36,37]), glass [38] and rubber from scrap tyres [39,40].

The research conducted so far about the fire behaviour of CPWA is very limited. As mentioned above, this is a topic worthy of investigation due to the combustible nature of this type of aggregate, its relatively low decomposition temperature and the consequent possible influence on the residual mechanical performance. To the authors' best knowledge, the only study reported in the literature addressing the fire behaviour of CPWA is the one by Albano et al. [8]. These authors investigated the residual flexural strength of concrete slabs incorporating PET waste as a replacement of natural fine aggregate after being exposed to temperatures of 200 °C, 400 °C and 600 °C for 2 h. The authors tested several concrete mixes (that exhibited different slumps) in which they varied the w/c ratio (0.50 and 0.60), the replacement ratio (10% and 20%) and the size of the PET particles (0.26 cm, 1.14 cm and a 50/50 combination thereof). Regardless of the composition, the flexural strength of all concrete mixes suffered no noticeable changes after being exposed to 200 °C, but presented a considerable decrease after being subjected to 400 °C and especially after being exposed to 600 °C. The authors did not provide a comparison of the performance reduction (with temperature) of the different CPWA mixes with that experienced by reference concrete mixes. Furthermore, in this study, the effects of PET waste incorporation on the residual compressive and tensile strengths as well as on the elastic modulus were not determined.

This paper aims at bridging the current gap in the information about the behaviour of CPWA subjected to elevated temperatures. In particular, this study is focused on the assessment of the thermal response and post-fire residual mechanical properties of CPWA (compared to normal concrete), namely the compressive and splitting tensile strengths, the elastic modulus, the ultrasonic pulse velocity, the surface hardness and the water absorption by immersion.

3. Experimental programme

3.1. Materials

The materials used in the experimental programme comprised natural aggregates (NAs), selected plastic waste aggregates (PWAs), cement type CEM II A-L 42.5 R (provided by SECIL), and tap water. The NAs (provided by Unibetão) included crushed limestone of three size ranges used as coarse aggregates, and quartzite river sand of two size ranges used as fine aggregates. Three types of PET PWAs (provided by Selenis, a plastic recycling plant) were used: coarse and flaky (PCAs – plastic coarse aggregates), fine and flaky (PFAs – plastic fine aggregates), and fine and regular shape (PPAs – plastic pellet aggregates). PCAs and PFAs were obtained by shredding PET bottles to particles with sizes between 2 mm and 11.2 mm and 1 mm and 4 mm, respectively. PPAs resulted from a thermal treatment of shredded PET bottle waste.

3.2. Tests on aggregates

The following tests were carried out on the different types of aggregates: (i) size grading analysis, in accordance with EN 933-1 [41] and EN 933-2 [42]; (ii) particle density and water absorption (EN 1097-6 [43]); (iii) loose bulk density (EN 1097-3 [44]); (iv) Los Angeles abrasion (only for the coarser NA, LNEC E-237 [45]); and (v) shape index (EN 933-4 [46]). Table 1 shows the most relevant results of these tests and Fig. 1 illustrates the grading curves of the NAs and PWAs used in the experiments.

The particle dry density of PWAs is significantly lower than that of NAs. The same applies to bulk density, but here there is a remarkable difference between the values of the various types of PWAs, with maximum and minimum values presented respectively by PPA (739 kg/m^3) and PCA (261 kg/m^3) aggregates. This stems from the PCA aggregates' flaky shape, which determines a less efficient space use. The water absorption results show a similarity between PWAs and NAs. The water absorption of PWAs (which, in principle, should be impermeable) was slightly higher than that reported in the literature (e.g., [5,9,10]), possibly due to the difficulty in drying completely the aggregates' surface.

The mass variation and energy changes as a function of temperature suffered by the three types of PWAs were also evaluated by means of thermogravimetric (TGA) and differential scanning calorimetry (DSC). Tests were carried out according to ISO 11357 [47] on *a SDT2960 Simultaneous* thermogravimetric analyser from *TA Instruments* from ambient temperature (approximately 20°) to about 800 °C in air atmosphere, at a heating rate of 5 °C/min. Fig. 2 shows the remaining mass (RM) and the heat flow (HF) of the PWAs as a function of temperature. The behaviour exhibited by the three types of PWAs is very similar. Up to approximately 350 °C, PWAs suffer some kind of decomposition, with reduced mass loss and very little thermal effects. For higher temperatures, PWAs ignite and burn – the remaining mass decreases very sharply and the heat flow curves exhibit considerable exothermic peaks. The average onset decomposition temperature (for the three types of PWAs), defined as the temperature for which 5% of the mass is lost, was set at $T_{d,\text{onset}}$ = 378 °C. The average temperature of decomposition, determined as the temperature for which 50% of the mass is lost, was set as T_d = 425 C. For temperatures higher than about 550 °C, the mass remained constant, with an average final inorganic residual mass of 0.2%.

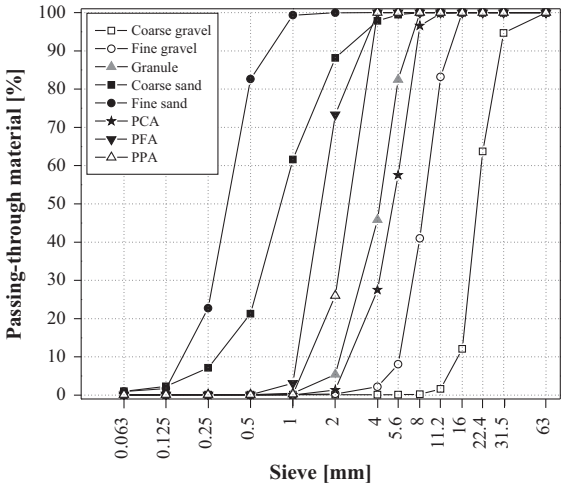

Fig. 1. Grading curves of the NAs and PWAs used in the concrete mixes.

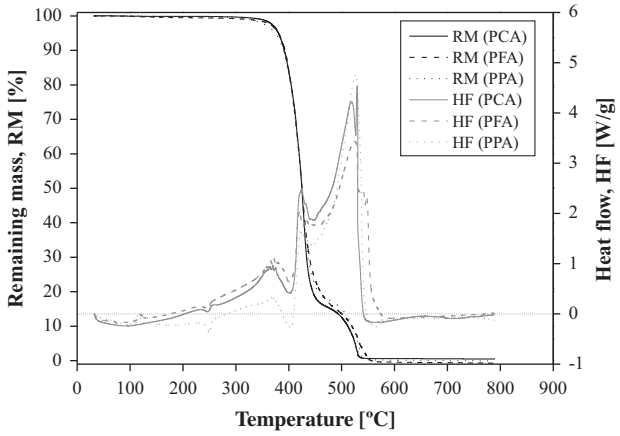

Fig. 2. TGA/DSC tests on PWAs: remaining mass and heat flow *vs.* temperature.

3.3. Concrete mixes design

The experimental programme comprised the design of a total of six concrete mixes: a reference concrete (RC), a concrete mix with an NA/PCA replacement ratio of 7.5% (referred to as C7.5PC), two concrete mixes with NA/PPA replacement ratios of 7.5% and 15% (C7.5PP and C15PP), and finally two concrete mixes with NA/PFA replacement ratios of 7.5% and 15% (C7.5PF and C15PF).

The composition of all mixes is shown in Table 2. The RC was designed according to Faury's method [48] aiming at a compressive strength class C30/37 (according to EN 206-1 [49]) with a slump of 125 ± 10 mm. The maximum particle size was set as 22.4 mm. This resulted in a cement content of 350 kg/m^3 and a w/c ratio of 0.54. No admixtures or additional constituents were used.

Regarding the CPWA mixes, in order to allow a valid comparison between the results of each composition, the Abrams cone slump of all mixes was also set equal to 125 ± 10 mm. In addition, all mixes in this experiment have the same aggregate size distribution and cement content. The different influence of each type of PWA in the workability of fresh concrete, associated to its replacement ratio, imposed an adjustment of the w/c of each mix. The replacement of NAs by flaky PWAs (PCAs and PFAs) caused a reduction of the slump values, more pronounced for the highest incorporation ratio, resulting in a w/c increase to regain the target slump. On the other hand, the more spherical shape of PPAs in comparison to the NAs allowed a reduction of the w/c.

Table 1
Aggregate test results.

Type of aggregate	Coarse gravel	Fine gravel	Granule	Coarse sand	Fine sand	PCA	PPA	PFA
Particle dry density (kg/m^3)	2671	2665	2732	2717	2647	1302	1303	1280
Water absorption (%)	0.55	0.92	0.31	0.05	0.15	0.75	0.39	0.11
Loose bulk density (kg/m^3)	1394	1420	1469	1461	1462	261	739	438
Los Angeles coefficient (%)	32.0	29.3	–	–	–	–	–	–
Shape index (%)	11.0	16.2	–	–	–	–	–	–

Table 2
Composition, w/c ratio, fresh density, slump, and 28-day mechanical properties of all concrete mixes (average ± standard deviation).

Component/property		Concrete mix					
		RC	C7.5PC	C7.5PF	C15PF	C7.5PP	C15PP
Natural coarse aggregates (kg/m^3)	16–22.4 mm	323.0	311.3	319.6	313.0	324.6	328.0
	11.2–16 mm	321.2	309.6	317.8	311.2	322.8	326.1
	8–11.2 mm	122.8	113.2	121.5	119.0	123.4	124.7
	5.6–8 mm	125.5	60.9	124.2	121.6	126.1	127.4
	4–5.6 mm	110.7	60.0	109.6	107.3	111.3	112.4
Natural fine aggregates (kg/m^3)	2–4 mm	204.8	176.1	127.4	51.0	102.9	0.0
	1–2 mm	164.0	158.0	105.2	47.2	131.3	98.9
	0.5–1 mm	102.5	98.8	101.4	99.3	103.0	104.1
	0.25–0.5 mm	257.0	247.7	254.4	249.1	258.3	261.0
	0.125–0.25 mm	72.4	69.8	71.7	70.2	72.8	73.5
PCA (kg/m^3)	8–11.2 mm	0	2.5	0	0	0	0
	5.6–8 mm	0	27.6	0	0	0	0
	4–5.6 mm	0	21.5	0	0	0	0
	2–4 mm	0	9.8	0	0	0	0
PFA (kg/m^3)	2–4 mm	0	0	35.3	69.1	0	0
	1–2 mm	0	0	28.9	56.6	0	0
PPA (kg/m^3)	2–4 mm	0	0	0	0	49.5	100.0
	1–2 mm	0	0	0	0	17.4	35.1
Cement (kg/m^3)		350	350	350	350	350	350
Water (kg/m^3)		189	214	186	179	196	210
w/c ratio (–)		0.54	0.61	0.56	0.60	0.53	0.51
Slump (mm)		127 ± 4.2	116 ± 2.2	130 ± 8.4	127 ± 10.3	128 ± 5.4	124 ± 8.8
Fresh density (kg/m^3)		2401 ± 19.2	2293 ± 19.1	2347 ± 12.7	2275 ± 16.7	2319 ± 11.4	2204 ± 24.0
$f_{cm,28}$ (MPa)		44.0 ± 1.10	29.3 ± 0.50	38.6 ± 1.81	36.3 ± 1.02	34.7 ± 0.42	27.5 ± 0.80
$f_{ctm,28}$ (MPa)		2.82 ± 0.21	2.28 ± 0.12	2.50 ± 0.31	2.02 ± 0.16	2.27 ± 0.13	1.76 ± 0.28
$E_{cm,28}$ (GPa)		34.8 ± 2.85	26.8 ± 0.59	31.8 ± 0.83	28.8 ± 0.58	29.8 ± 0.42	21.9 ± 0.92

3.4. Specimen preparation

For all concrete mixes and the four conditions tested (28 days, ambient temperature exposure (T20) and two values of elevated temperature exposure (T600 and T800), *cf.* Section 3.6), 5 cubic specimens (150 mm) were produced for compressive strength tests, while 5 and 3 cylindrical specimens (φ150 × 300 mm) were produced respectively for splitting tensile strength and elastic modulus tests. For test conditions T20, T600 and T800, 3 additional cubic specimens (150 mm) were produced for water absorption by immersion tests.

The samples were demoulded 24 h after casting and placed in a wet curing chamber (temperature of T = 20 °C and relative humidity of RH = 100%) until 28 days. The specimens used for fire behaviour characterization (conditions T20, T600 and T800) were then moved to a dry chamber (T = 20 ± 2 °C and RH = 50 ± 5%) where they remained for further 49 days.

3.5. Tests on fresh concrete

The fresh concrete was characterized in what concerns its (i) slump, determined by means of the Abrams cone test (EN 12350-2 [50]), and (ii) fresh density (EN 12350-6 [51]). Results obtained, presented in Table 2, show that the slump of all mixes remained within the established range (125 ± 15 mm), thereby allowing a valid comparison of the results of the various mixes. As mentioned above, this was accomplished at the expense of adjusting the w/c ratio, which was increased in mixes C7.5PC, C7.5PF and C15PF (due to the flakier shape of PCAs and PFAs) and was decreased in mixes C7.5PP and C15PP (due to the regular shape, smooth texture and impermeable nature of PPAs). As expected, the incorporation of PWAs caused a reduction of the fresh density, due to the lower particle density of PWAs in comparison to NAs. Accordingly, the magnitude of this reduction increased with the replacement ratio. The different reductions obtained in the various types of PWAs stem mainly from the differences in the w/c of each mix.

3.6. Thermal exposure

In order to assess the post-fire residual mechanical properties of CPWA, each type of concrete was subjected to the following thermal treatments: 20 °C (T20, reference exposure), 600 °C (T600) and 800 °C (T800), the last two for a period of 1 h (the values mentioned refer to the air temperature inside the furnace). Specimens subjected to exposures T600 and T800 were heated in a vertical oven (external dimensions of 1.35 m long × 1.20 m wide × 2.10 m high) fired by six gas burners controlled by a computer, which reads the oven temperature from three internal thermocouples and is able to adjust the burners' intensity in order to follow, as close as possible, a predefined time–temperature curve. In this study, heating was performed with the fire exposure defined in the ISO 834 standard [14], also referred in Eurocode 1 – part 1.2 [52],

$$T(t) = 20 + 345 \times \log_{10}(8 \times t + 1) \quad (1)$$

where T is the oven temperature (°C) and t is the time (min).

The nominal heating time–temperature curves (T600 and T800) used for each exposure temperature are plotted in Fig. 3. As the main goal of the present study was not to perform a full and thorough characterization of the post-fire residual mechanical performance of CPWA (nor of the fire resistance of members made with it), but rather to assess the direct influence of incorporating PWA on such performance, it was decided to combine the rapid heating of ISO 834 standard curve ([14], which encompasses a rapid heating) with the temperature plateau (in this case, at 600 °C and 800 °C, respectively) specified by RILEM TC 129-MHT [53]. This procedure was adopted in several other comparative studies (e.g., [15,18,29,32]).

Cooling of the specimens took place slowly inside the oven until temperatures decreased to around 200 °C, after which the oven door was opened and the specimens were moved to a controlled chamber (T = 20 ± 2 °C and RH = 50 ± 5%), where they remained for at least 4 days prior to any further characterisation tests (*cf.* Section 3.7).

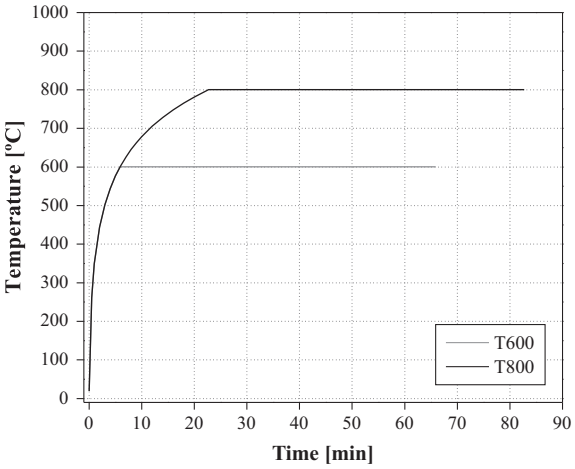

Fig. 3. Time–temperature curves for thermal exposures T600 and T800.

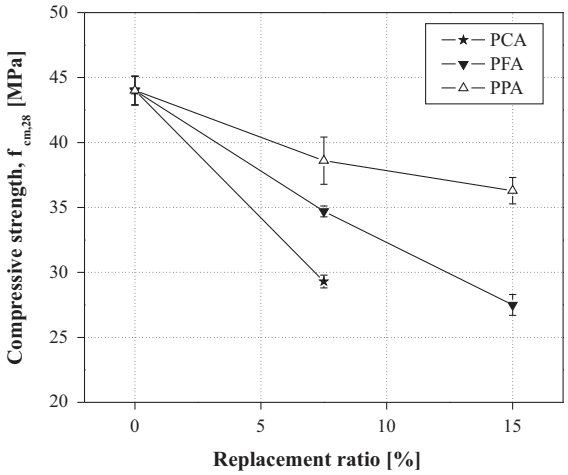

Fig. 4. 28-day compressive strength *vs.* ratio of replacement of NAs by RWAs (average ± standard deviation).

Due to the considerable amount of material to be heated and the limited dimensions of the oven, each thermal exposure had to be carried out in three batches, which included (i) specimens from mixes RC and C7.5PC, (ii) specimens from mixes C7.5PP and C15PP, and (iii) specimens from mixes C7.5PF and C15PF.

During heat exposure, thermocouples type-K were used to measure the temperature evolution at three different depths of dummy cubic specimens of each concrete composition: 0 mm (thermocouple T1), 37.5 mm (T2), and 75 mm (T3).

3.7. Tests on hardened concrete

To evaluate and compare the post-fire mechanical properties of the various concrete mixes, compressive strength tests (according to EN 12390-3 [54]), splitting tensile strength tests (EN 12390-6 [55]) and elastic modulus tests (LNEC E 397 [56]) were carried out at 28 days, as well as before and after fire exposure.

As a complement to the above mentioned tests, all concrete mixes were subjected to the following additional tests before and after fire exposure: (i) ultrasonic pulse velocity (UPV) tests (EN 1250-4 [57]); (ii) surface hardness tests (EN 12504-2 [58]); and (iii) water absorption by immersion tests (LNEC specification E394 [59]). The UPV tests were performed on the cubic specimens used for compressive strength tests using a *PUNDIT* UPV equipment. The surface hardness tests were performed on the same specimens using a Schmidt concrete testing hammer. These three complementary tests comprise expeditious and non-destructive characterisation procedures. The main goal in performing these tests was (i) to complement the characterisation of the fire behaviour of CPWA and especially (ii) to evaluate the feasibility of using these techniques as indirect characterisation tests in the scope of *in situ* surveys of fire damaged structures. To this end, the correlation between the results obtained with these techniques and residual compressive strength was evaluated.

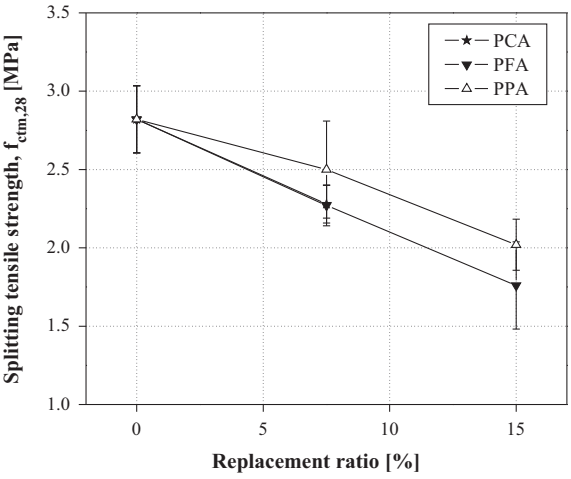

Fig. 5. 28-day splitting tensile strength *vs.* ratio of replacement of NAs by RWAs (average ± standard deviation).

4. Results and discussion

4.1. Mechanical properties at 28 days

The average compressive strength ($f_{cm,28}$), splitting tensile strength ($f_{ctm,28}$) and elastic modulus ($E_{cm,28}$) at 28 days of the concrete compositions (without any fire exposure) are plotted in Figs. 4–6, respectively. As expected, the replacement of NA by PWA resulted in a decrease of all mechanical properties, more pronounced for higher incorporation ratios. The deterioration of

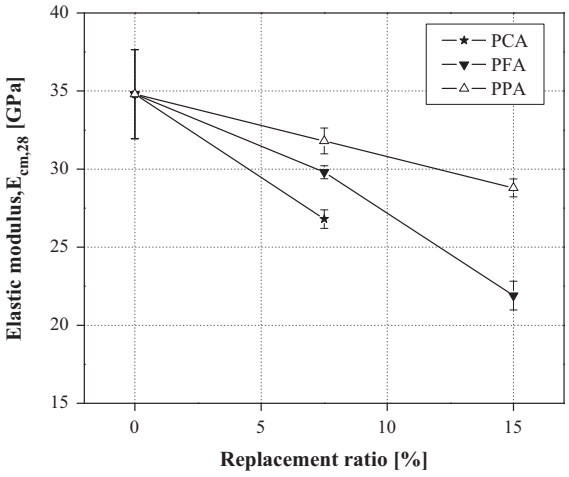

Fig. 6. 28-day elastic modulus *vs.* ratio of replacement of NAs by RWAs (average ± standard deviation).

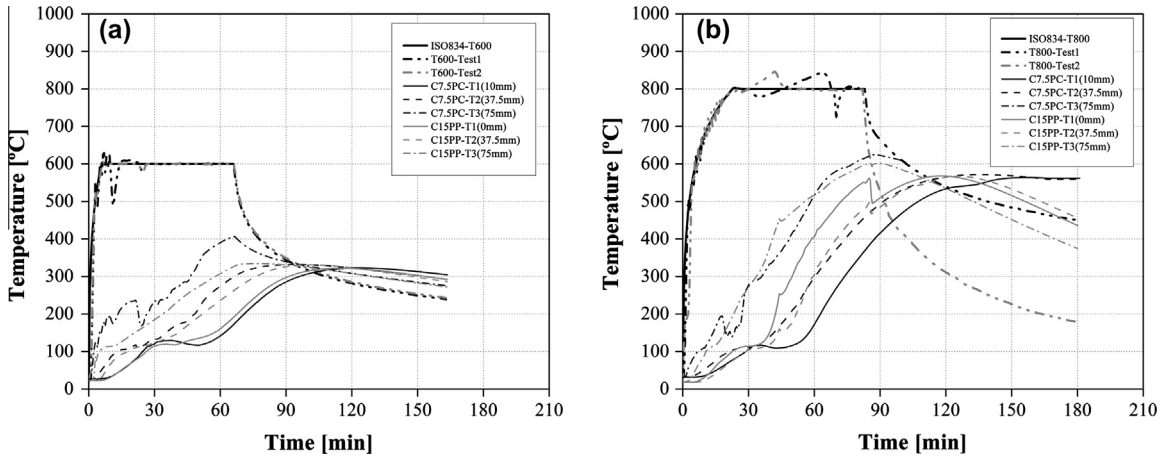

Fig. 7. Time–temperature curves inside the oven and at different depths of the specimens for each thermal exposure: (a) T600 and (b) T800.

mechanical performance with PWA incorporation stems from (i) the significantly lower stiffness of PWA compared to NA and (ii) the weak bond between these recycled aggregates and the cement paste. Apart from their smooth surface, which results in a weak macroscopic bond, the low porosity of PWA does not allow the impregnation and subsequent crystallization of the binder therein. For similar replacement ratios, the different types of PWA cause varying reductions in the mechanical performance. This can be explained by their different shape and size, the corresponding influence on concrete's workability and consequent different needs to adjust the w/c ratio (to keep the slump constant).

4.2. Thermal response

Fig. 7 shows the evolution of temperatures inside the oven and at different depths of specimens of concrete compositions C7.5PC and C15PP, for T600 and T800 thermal exposures, respectively. For the two different types of thermal exposure used in the experimental programme, the qualitative temperature profiles were roughly similar for all concrete compositions. During the heating phase temperatures inside the test specimens increased gradually, at a slower rate when compared with the increase in the oven temperature. During this first stage, temperatures increased from the surface to the core. After the oven was turned off, the temperature gradient inside the test specimens was remarkably reduced, i.e. temperatures became much more uniform across the specimens' depth.

Fig. 8 shows the maximum average temperatures reached in the different types of specimens, for the two thermal exposures T600 and T800. The incorporation of PWAs in concrete resulted in an increase of the temperatures inside the test specimens – the maximum average temperatures reached in all concrete compositions with incorporation of PWAs were higher than those measured in the reference concrete. Furthermore, for each type of PWA, the magnitude of this difference increased with the incorporation ratio. The following two reasons explain this diverse thermal behaviour: (i) the higher porosity increase due to the replacement of NAs by PWAs, which facilitated the propagation of heat inside the concrete specimens, and (ii) the exothermic thermal decomposition of plastic aggregates that generates additional heat.

4.3. Visual observations

During heat exposure, it was not possible to observe the test specimens, as the furnace walls are opaque. However, after removal from the furnace, specimens were subjected to a thorough

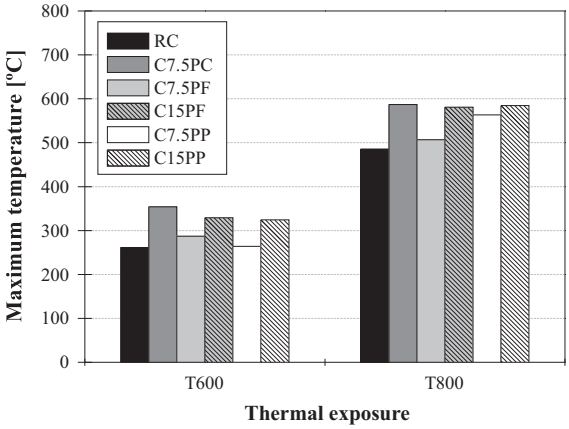

Fig. 8. Maximum internal temperatures for each thermal exposure: (a) T600 and (b) T800.

visual examination and compared with unheated specimens. In general, following thermal exposure, all specimens presented cracks on their surface – as expected, the length and width of these cracks increased with the exposure temperature. A limited number of specimens (at most, one per composition) subjected to both T600 and T800 thermal exposures exhibited signs of spalling, most often localized at the corners of those test specimens (preventing them from being tested). The surface colour of the specimens also underwent considerable changes – RC specimens became brighter (due to water loss), while CPWA specimens generally presented brown/black stains, especially for the T600 exposure, owing to the incomplete combustion of some plastic waste particles (for T800 exposure, such decomposition was much more complete). The surface of the CPWA specimens also presented extensive voids, corresponding to the decomposed plastic waste particles. For similar compositions, the number of voids was higher for T800 exposure, compared to T600 exposure, because the fraction of particles that underwent complete decomposition was higher for the former thermal exposure.

After performing the splitting tensile strength tests, it was possible to observe the full depth of all types of specimens (all compositions and thermal exposures) – Fig. 9 illustrates those observations. As expected, for thermal exposures T600 and T800, the natural aggregates exhibited pink/red discoloration, as they were heated up to temperatures ranging between 300 °C (T600) and 600 °C (T800). Fig. 9 also confirms that the degree of decomposition of the PWAs increased with temperature. In fact, while for

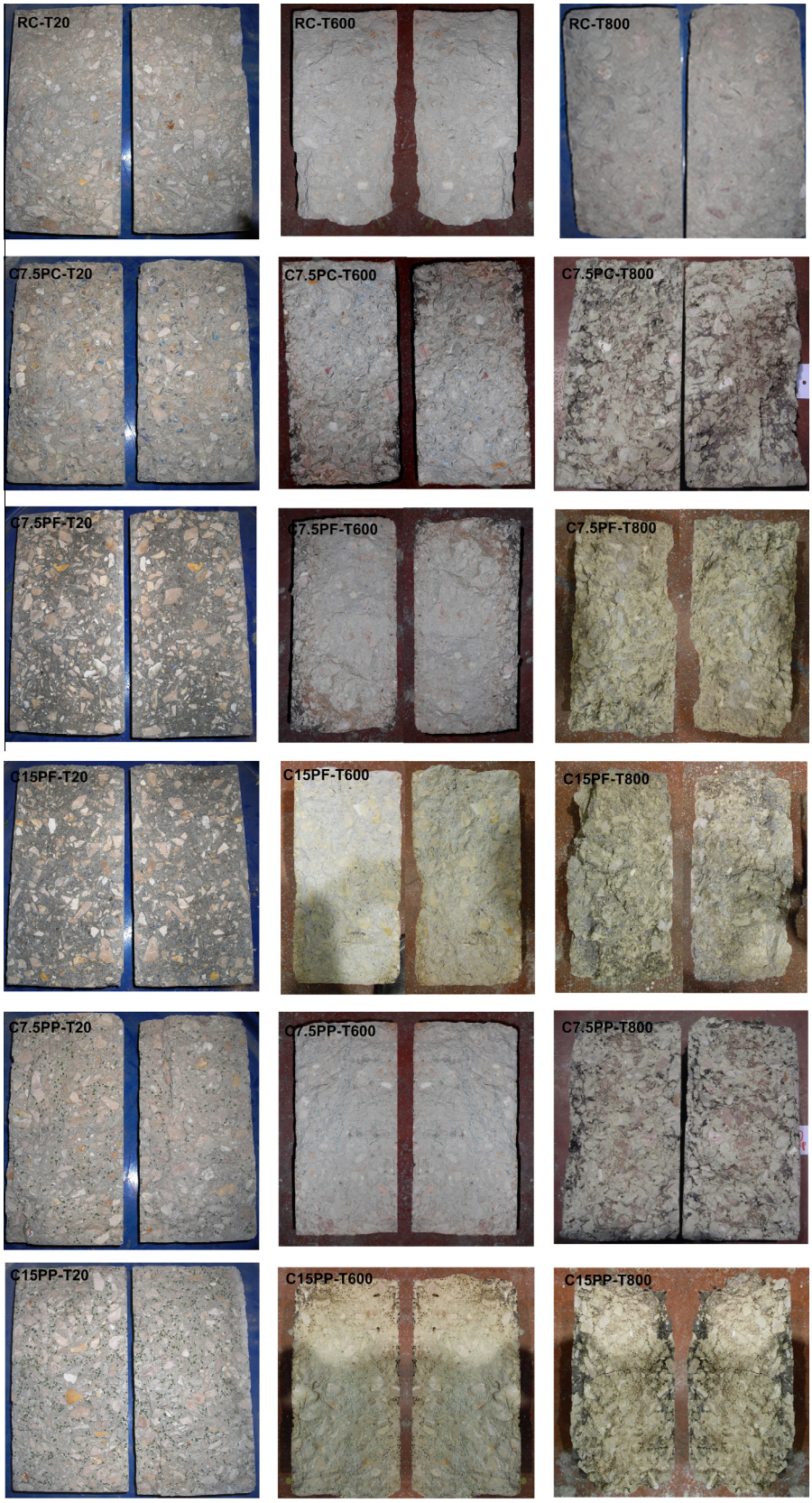

Fig. 9. Internal view of specimens from all compositions and thermal exposures, after the splitting tensile strength test.

specimens subjected to T600 exposure, there are still several PWA particles visible, for T800 exposure those particles are no longer present. These observations are consistent with results of thermogravimetric experiments (Fig. 2), in which a decomposition temperature of 425 °C and very low residual mass at 550 °C were determined.

4.4. Post-fire physico-mechanical performance

Table 3 shows the mechanical and physical properties of each type of concrete, for the different thermal exposure conditions. In addition, for each mix and test condition, the percentage deviation from RC (Δ_{RC}) is also listed.

4.4.1. Compressive strength

Fig. 10 plots for all concrete compositions the ratio between the residual compressive strength after exposure to elevated temperature (f_c^T) and the corresponding strength for the reference temperature of 20 °C (f_c^{20}) – results are presented as a function of both the exposure temperature (T_{oven}) and the average maximum internal temperature (T_{max}) reached by the specimens at different depths. Fig. 10 also plots the reduction curve for standard strength concrete made of limestone natural aggregate proposed by ASCE [60] and ACI [61], referring to concrete specimens tested in an "unstressed residual" condition, i.e. heated without being loaded and tested in compression after being cooled down. One should note that those reduction factors were obtained for specimens heated at a much lower rate compared to the present study – thereby, such reduction factors are plotted only as a comparative reference, since they refer to concrete specimens uniformly heated throughout their cross-section up to a given temperature (the temperature values for these curves refer to the concrete temperature).

For all concrete compositions there is an overall reduction of residual compressive strength after fire exposure, due to the physical–chemical reactions underwent by the different constituents of concrete at elevated temperature, as well as the effects of the thermal gradients developed during the heating stage. As expected, the magnitude of such reduction increases with the exposure temperature. It can also be seen that for similar temperatures our experimental results in terms of temperatures reached by the specimens (T_{max}) are lower than the ASCE [60] and ACI [61] reference curves, as the latter are much less influenced by thermal gradients.

Results indicate an increase of the compressive strength degradation with the replacement of NAs by PWAs. Such increased degradation of CPWA compared to RC is more pronounced for exposure T600, for which the average compressive strength of CPWA is already remarkably reduced (0.51 of residual compressive strength), whereas that of RC suffers only a moderate reduction (0.75 of residual compressive strength). For exposure T800, those figures become closer, respectively 0.29 and 0.24. The higher degradation of CPWA stems from the thermal decomposition of plastic aggregates, which results in a higher increase of concrete porosity (with large voids), hence in higher reduction of compressive strength. Moreover, such higher porosity decreases the resistance of concrete to the propagation of high temperatures, an effect that was confirmed by the temperatures measured within the samples (cf. Section 4.2). In addition, the exothermic combustibility of plastic aggregates also increases the thermal exposure.

Regarding the influence of the type of PWAs, the most relevant differences within CPWA mixes with similar replacement ratios

Table 3
Mechanical and physical properties of each type of concrete (average, $\bar{x}$ ± standard deviation, s) for the different thermal exposures and relative percentage difference to reference concrete (Δ_{RC}).

Property	Concrete mix	T20		T600		T800	
		$\bar{x} \pm s$	Δ_{RC} (%)	$\bar{x} \pm s$	Δ_{RC} (%)	$\bar{x} \pm s$	Δ_{RC} (%)
Compressive strength, f_c (MPa)	RC	48.7 ± 1.17	–	36.6 ± 3.04	–	15.5 ± 2.93	–
	C7.5PC	33.7 ± 0.88	−31	19.6 ± 4.45	−46	7.7 ± 1.45	−51
	C7.5PF	41.7 ± 1.25	−14	22.3 ± 2.43	−39	8.6 ± 3.37	−45
	C15PF	32.4 ± 0.58	−33	15.8 ± 5.10	−57	5.8 ± 1.49	−62
	C7.5PP	43.8 ± 2.85	−10	20.6 ± 3.38	−44	12.7 ± 5.40	−18
	C15PP	42.3 ± 0.89	−13	18.6 ± 2.94	−49	12.9 ± 4.17	−17
Splitting tensile strength, f_{ct} (MPa)	RC	3.62 ± 0.76	–	2.04 ± 0.09	–	0.66 ± 0.12	–
	C7.5PC	2.29 ± 0.25	−37	1.35 ± 0.22	−34	0.54 ± 0.22	−18
	C7.5PF	2.59 ± 0.41	−28	1.54 ± 0.40	−30	0.39 ± 0.23	−40
	C15PF	2.26 ± 0.14	−38	1.08 ± 0.31	−30	0.36 ± 0.10	−45
	C7.5PP	2.72 ± 0.23	−25	1.61 ± 0.36	−19	0.84 ± 0.25	28
	C15PP	2.24 ± 0.25	−38	1.19 ± 0.27	−26	0.54 ± 0.11	−19
Elasticity modulus, E_c (GPa)	RC	37.0 ± 0.89	–	20.2 ± 1.25	–	6.40 ± 1.18	–
	C7.5PC	25.5 ± 0.94	−31	12.2 ± 1.65	−39	4.40 ± 0.63	−30
	C7.5PF	32.2 ± 1.06	−13	13.7 ± 2.23	−32	3.70 ± 0.45	−43
	C15PF	24.8 ± 1.29	−33	9.50 ± 2.10	−53	2.80 ± 0.34	−56
	C7.5PP	34.3 ± 0.31	−7	17.6 ± 1.14	−13	4.50 ± 0.90	−29
	C15PP	29.4 ± 0.18	−21	12.6±	−38	3.80 ± 0.60	−40
Ultrasonic pulse velocity, UPV (m/s)	RC	4966 ± 10	–	3537 ± 615	–	1562 ± 456	–
	C7.5PC	4561 ± 59	−8	2736 ± 361	−23	1172 ± 356	−25
	C7.5PF	4515 ± 72	−9	3179 ± 245	−10	956 ± 272	−39
	C15PF	4150 ± 46	−16	2328 ± 549	−34	780 ± 131	−50
	C7.5PP	4945 ± 35	0	2659 ± 691	−25	923 ± 557	−41
	C15PP	4771 ± 48	−4	2747 ± 239	−22	916 ± 351	−41
Rebound number, N (–)	RC	33.5 ± 2.3	–	31.6 ± 3.0	–	21.3 ± 3.5	–
	C7.5PC	31.9 ± 0.9	−5	27 ± 3.1	−15	18.3 ± 1.9	−14
	C7.5PF	31.3 ± 0.8	−7	26.3 ± 0.6	−17	19.1 ± 3.4	−10
	C15PF	31.3 ± 1.0	−7	22.0 ± 4.0	−30	16.1 ± 1.4	−25
	C7.5PP	33.9 ± 0.5	1	30.9 ± 2.1	−2	22.9 ± 4.4	−7
	C15PP	35.6 ± 1.1	6	31 ± 3.1	−2	23.4 ± 3.0	10
Water absorption by immersion, W (%)	RC	13.9 ± 0.5	–	15.5 ± 4.7	–	19.3 ± 1.8	–
	C7.5PC	15.3 ± 1.3	10	17.6 ± 1.4	14	22.4 ± 2.3	16
	C7.5PF	13.8 ± 1.5	0	14.7 ± 0.2	−5	21.6 ± 0.7	12
	C15PF	12.6 ± 0.1	−10	13.6 ± 0.1	−12	22.3 ± 0.2	16
	C7.5PP	15.3 ± 1.6	10	15.3 ± 0.4	−1	22.9 ± 1.1	19
	C15PP	15.6 ± 0.4	13	16.4 ± 0.6	6	27.0±0.9	40

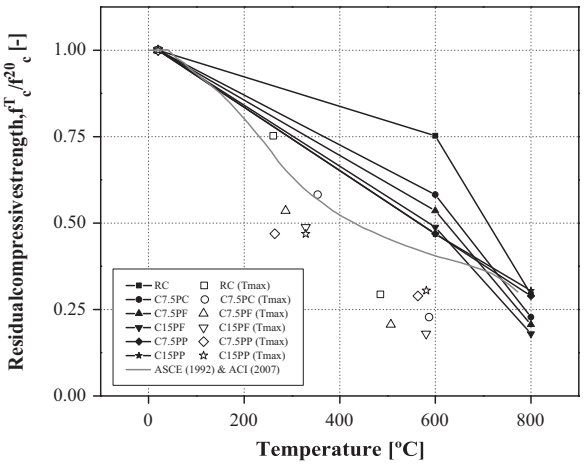

Fig. 10. Residual compressive strength: comparison between the results obtained in this study (as a function of the oven temperature and average maximum temperature in the specimens), and the reference values of ASCE [60] and ACI [61].

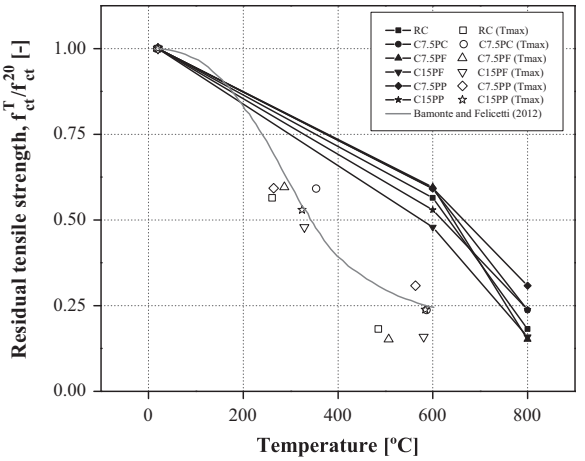

Fig. 11. Residual tensile strength: comparison between the results obtained in this study (as a function of the oven temperature and average maximum temperature in the specimens), and the reference values of Bamonte and Felicetti [62].

were found following the exposure to 800 °C, for which the lowest degradation was obtained with PPAs. This trend is explained by (i) the different shape and size of the PWAs, which leads to distinct porosity distributions after exposure to elevated temperature (more uniform and with smaller voids in mixes incorporating PPAs), and (ii) the different w/c ratios of these mixes. In general, the replacement ratio increase of 7.5% to 15% had limited influence on the reduction of residual compressive strength; such influence was more visible for PFAs incorporation. It is likely that the deterioration of compressive strength due to increased porosity (owing to the thermal decomposition of PWAs) is compensated to some extent by the better accommodation of thermal expansions provided by the voids created. Furthermore, this higher porosity also allows confined gases to escape, thereby reducing the build-up of internal stresses and, hence, concrete cracking (this effect being more important in tensile strength, *cf*. Section 4.4.2.). As mentioned, the attenuation of the effects of replacing NAs by PWAs in the degradation of compressive strength are more evident for exposure T800, for which the thermal decomposition of the PWAs and the thermal expansion of the constituents of the concrete are considerably more pronounced than for exposure T600.

4.4.2. Splitting tensile strength

The ratio between the residual splitting tensile strength after exposure to elevated temperature (f_{ct}^{T}) and the corresponding strength for the reference temperature of 20 °C (f_{ct}^{20}) is illustrated in Fig. 11 – as for compressive strength, splitting tensile strength results are presented as a function of both the exposure temperature (T_{oven}) and the average maximum internal temperature (T_{max}) reached by the specimens at different depths. The reduction curve for standard strength concrete proposed by Bamonte and Felicetti [62] are also plotted in Fig. 11 as a reference, since it was obtained for different test in different conditions (specimens heated at slow rate).

For all concrete compositions, there is an overall reduction of the splitting tensile strength after exposure to elevated temperatures and, as expected, the magnitude of such reduction increases with the exposure temperature. Unlike compressive strength, the incorporation of PWAs did not result in an increase of the degradation of residual splitting tensile strength. In fact, while for exposure T600 the average degradation of CPWA compositions was roughly similar to that of RC (0.56 of residual splitting tensile strength), for the most severe thermal exposure T800 the average residual splitting tensile strength of CPWA mixes was even slightly higher than that of RC (0.22 *vs*. 0.18). This improved behaviour in tension may be explained by the already mentioned favourable effects stemming from the higher porosity of CPWA: besides mitigating the accumulation of internal stresses due to the thermal incompatibility of concrete constituents, it also allows the dispersion of gases confined in pores, thereby reducing crack development. Unlike compressive strength, it is very likely that any detrimental effects caused by the voids had less influence than the reduction in crack development within the concrete matrix promoted by the porosity increase.

Similarly to compressive strength, the lowest tensile strength reductions were obtained with the incorporation of PPAs, particularly for the highest exposure temperature. In addition, higher replacement ratios generally caused increasing degradation of tensile strength.

The splitting tensile strength results obtained in our study in terms of the maximum temperatures reached by the specimens seem to follow the overall variation trend reported by Bamonte and Felicetti [62]. Due to the aforementioned reasons, our experimental data is generally lower than that reported by those authors.

4.4.3. Elastic modulus

Fig. 12 presents the ratio between the residual elastic modulus after exposure to elevated temperature (E_c^T) and the corresponding elastic modulus for the reference temperature of 20 °C (E_c^{20}) for all concrete compositions. As for the previous mechanical properties, results are presented as a function of both the exposure temperature (T_{oven}) and the average maximum internal temperature (T_{max}) reached by the specimens at different depths. Fig. 12 plots also an intermediate reduction curve obtained by Phan and Carino [63] for standard strength concrete made of limestone natural aggregate subjected to slow heating.

The elastic modulus of all compositions tested was remarkably reduced after exposure to elevated temperatures. The degradation increased with the exposure temperature according to the general variation trend reported by Phan and Carino [63]. Similarly to the other properties, and due to the same reasons, our experimental data are generally lower than that reference curve. Furthermore, for similar exposure temperatures, the elastic modulus suffered higher reduction than the compressive and splitting tensile strengths, which is consistent with previous studies reported in the literature on conventional concrete (e.g., [64]). The greater reduction in this mechanical property is due to its higher

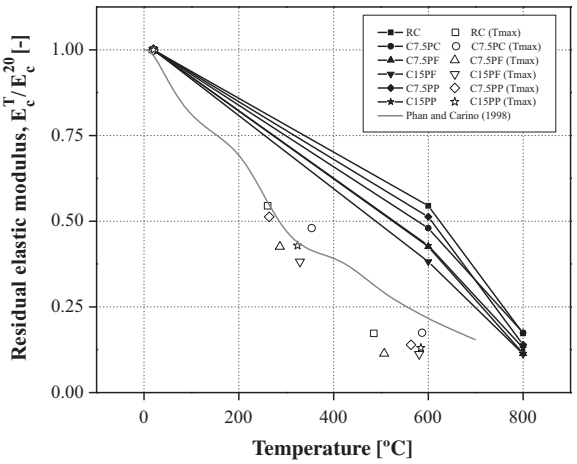

Fig. 12. Residual elastic modulus: comparison between the results obtained in this study (as a function of the oven temperature and average maximum temperature in the specimens) and the reference values of Phan and Carino [63].

susceptibility to concrete cracking, which is intensified with increasing thermal exposure.

Results obtained show that the degradation of the elastic modulus experienced by concrete with PWA is more pronounced than that of reference concrete: the average residual elastic moduli among the different CPWA mixes after exposure to 600 °C and 800 °C were respectively 0.45 and 0.13, which compare with 0.54 and 0.17 for the RC. Furthermore, the elastic modulus reduction consistently increased with the replacement ratio of NA by CPWA. Following thermal exposure, the (large) voids created by the thermal decomposition of plastic waste aggregate explain the increased loss of stiffness of CPWA mixes.

Regarding the influence of the type of PWAs and the replacement ratio, the results of elastic modulus are consistent with those of compressive strength, i.e. PPAs lead to the lowest performance reduction, whereas a higher replacement ratio causes increasing degradation, particularly for T600 exposure.

4.4.4. Ultrasonic pulse-velocity

Fig. 13 shows for all concrete compositions the ratio between the residual ultrasonic pulse velocity after exposure to elevated temperature (UPV^T) and that for the reference temperature of 20 °C (UPV^{20}). The residual UPV followed the same overall variation with temperature as compressive strength (*cf.* Fig. 10). In addition, the incorporation of PWAs resulted in increased reduction of UPV compared to the RC, particularly for the highest exposure temperature, and this reduction increased with the replacement ratio. These results are explained by the increased porosity of concrete stemming from the decomposition of PWAs.

Fig. 14 plots the correlation between the UPV and the compressive strength for all concrete compositions and exposure conditions. The (linear) relationship between those properties is statistically significant (R^2 = 0.862), thereby indicating the suitability of determining the UPV as an expeditious and non-destructive test to estimate the residual compressive strength of CPWA exposed to fire.

4.4.5. Surface hardness (rebound index)

Fig. 15 shows the ratio between the rebound index after exposure to elevated temperature (N^T) and that for the reference temperature of 20 °C (N^{20}). Although the scatter of surface hardness data was relatively high, all concrete compositions present an overall reduction trend with the exposure temperature. The results show a more severe deterioration with increasing PWA content. The reduction of the surface hardness is due to the chemical decomposition and cracking of the surface layer of concrete caused by the thermal exposure [65]. For CPWA, the combustion of plastic aggregate increases porosity, further weakening the surface layer of concrete.

Fig. 16 plots the correlation between the rebound number and compressive strength. In this case, the (linear) correlation

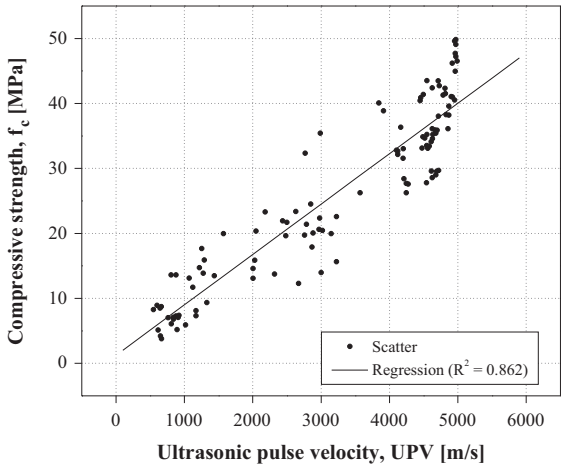

Fig. 14. Correlation between ultrasonic pulse velocity and compressive strength.

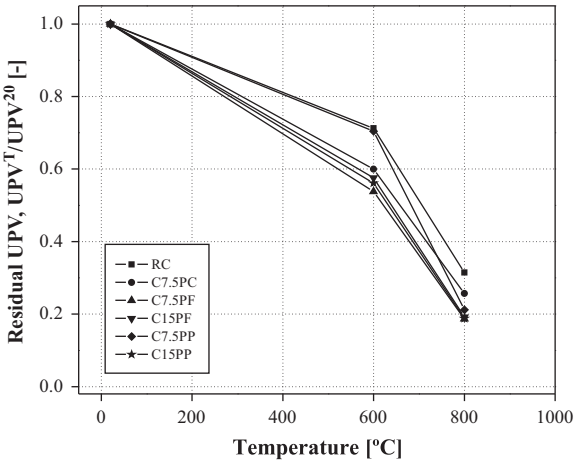

Fig. 13. Residual ultrasonic pulse velocity as a function of the oven temperature.

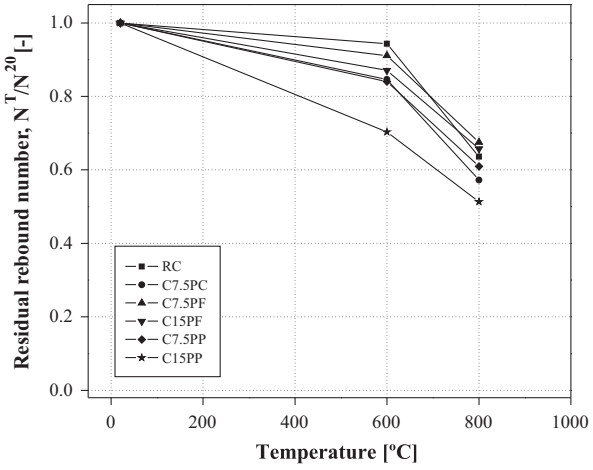

Fig. 15. Residual rebound number as a function of the oven temperature.

coefficient is not as high as that obtained for UPV (R^2 = 0.68, much lower than that corresponding to tests performed at 28 days, R^2 = 0.97), pointing out the limitations in using this test as a reliable technique to assess the post-fire compressive strength of CPWA. It is also worth mentioning that unlike the other non-destructive characterisation procedures (*cf.* Sections 4.4.4. and 4.4.6.), the scatter varied among the different CPWA compositions, being minimum for the PFA and maximum for the PPA, this being explained by the higher influence in the surface hardness of the size and distribution of voids, namely those near the concrete surface. In fact, for PPA compositions, voids are larger and in less number than PFA counterparts.

4.4.6. Water absorption by immersion

Fig. 17 depicts the ratio between the residual water absorption by immersion after exposure to elevated temperature (W^T) and that for the reference temperature of 20 °C (W^{20}). As expected, the residual water absorption increased with the exposure temperature for all concrete mixes. The replacement of NAs by PWAs only resulted in a clear increase of the water absorption by immersion for exposure T800. This can be explained by the almost complete combustion of the plastic aggregates following the exposure to 800 °C, which resulted in a significant increase of concrete porosity. Moreover, for exposure T600, the decomposition of plastic aggregates was partial and more concentrated on the surface layer of concrete specimens. Furthermore, to some extent, the water absorption of CPWA after exposure to 600 °C may have been limited by the cover of melted plastic, which partially water-tightened the surface layer of these samples.

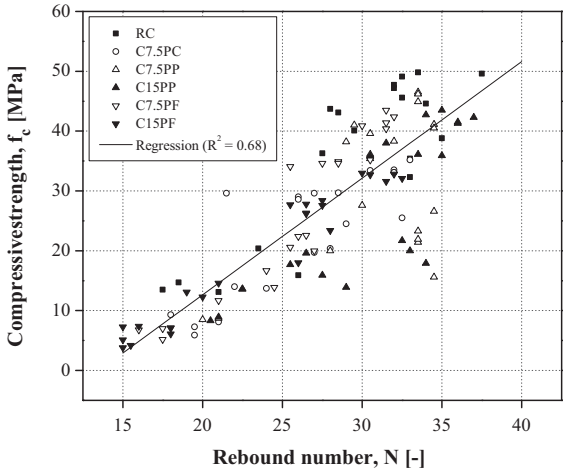

Fig. 16. Correlation between rebound number and compressive strength.

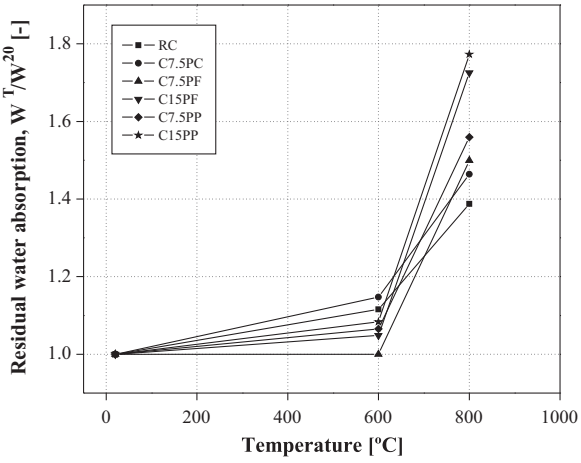

Fig. 17. Residual water absorption by immersion as a function of the oven temperature.

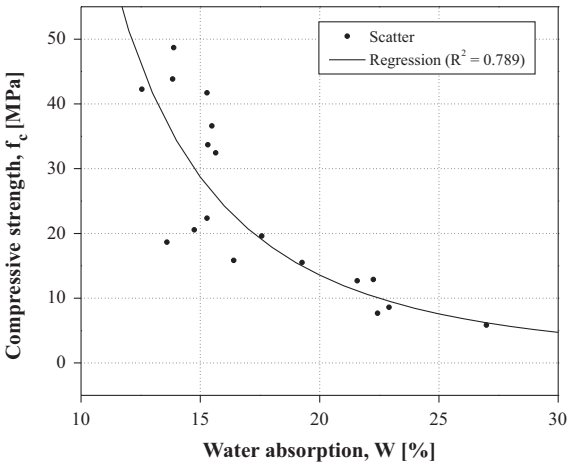

Fig. 18. Correlation between water absorption by immersion and compressive strength.

Fig. 18 shows the relationship between the average values of compressive strength and water absorption by immersion. There is a general good (power law) agreement between those properties. Concrete mixes which have suffered a higher thermal degradation and, thereby, have lower post-fire compressive strength, also exhibit higher water absorption by immersion. The relatively high correlation coefficient obtained suggests that water absorption by immersion is a reliable test to assess the residual compressive strength of fire-damaged CPWA.

5. Conclusions

This paper presented an experimental study on the performance of concrete made with PWAs as a replacement of NAs after exposure to elevated temperatures. The results obtained allow drawing the following main conclusions:

(1) The incorporation of PWAs as a replacement of NAs in ratios of 7.5% and 15% influences the thermal response of concrete exposed to elevated temperature. The maximum temperatures reached in CPWA are higher than those in RC, and this difference increases for higher replacement ratios. The different thermal behaviour of CPWA stems from (i) the higher increase of concrete porosity due to the replacement of NAs by PWAs, which facilitates heat propagation, and (ii) the exothermic thermal decomposition of PWAs that generates additional heat.

(2) The degradation suffered by CPWA after exposure to elevated temperature is, to some extent, similar to that of conventional concrete. Following heat exposure, specimens of all concrete compositions exhibited cracking, localized spalling and the typical colour changes due to the various physical–chemical changes suffered by the various concrete constituents. In addition, in CPWA mixes the thermal decomposition of PWAs created voids in the concrete matrix, causing considerable porosity increase.

(3) The degradation of compressive strength and elastic modulus of CPWA after exposure to elevated temperatures was higher than that of RC. This higher degradation of CPWA, which tended to increase with the replacement ratio, is

due to (i) the thermal decomposition of PWAs, which results in higher porosity of concrete and voids, as well as (ii) the development of higher temperatures in CPWA.

(4) In what concerns the splitting tensile strength, the incorporation of PWA did not affect the degradation of residual properties. It is possible that the higher porosity caused by the incorporation of PWAs attenuates the accumulation of internal stresses due to the thermal incompatibility of concrete constituents and allows the dispersion of gases confined in pores, thereby reducing crack development within the matrix. This effect seems to have been more relevant than any detrimental consequences due to the voids themselves.

(5) The magnitude of residual mechanical properties reduction was seen to depend on the type of PWAs incorporated in the concrete mix: the lower reductions were obtained with fine and regular shape aggregates (PPAs). In addition, for higher replacement ratios degradation generally increased.

(6) The residual compressive strength of CPWA was proved to be strongly correlated with both the ultrasonic pulse velocity and the water absorption by immersion. Therefore, these tests are deemed as adequate to be used as expeditious and non-destructive techniques to assess the residual compressive strength of CPWA in fire damaged structures. The correlation between compressive strength and surface hardness was less significant, highlighting the lower reliability of the rebound test to estimate the residual compressive strength of fire damaged structures made of CPWA.

Acknowledgements

The authors wish to thank ICIST, IST and FCT for funding the research, and companies Secil, Unibetão and Selenis for supplying the materials used in the experiments.

References

[1] European Association of Plastics Manufacturers (PlasticsEurope), Plastics – The Facts 2012. An analysis of European plastics production, demand and waste data for 2011. Brussels, 2012.
[2] Iadav I. Laboratory investigations of the properties of concrete containing recycled plastic aggregates. Patiala, India: Civil Engineering Department, Thapar University; 2008.
[3] Themelis NJ, Castaldi MJ, Bhatti J, Arsova L. Energy and economic value of nonrecycled plastics (nrp) and municipal solid wastes (msw) that are currently landfilled in the fifty states. Columbia University, Earth Engineering Center; 2011.
[4] Paszun D, Spychaj T. Chemical Recycling of Poly(ethylene terephthalate). Ind Eng Chem Res 1997;36:1373–83.
[5] Saikia N, de Brito J. Mechanical properties and abrasion behaviour of concrete containing shredded PET bottle waste as a partial substitution of natural Aggregates. Constr Build Mater 2014;52:236–44.
[6] Ferreira L, de Brito J, Saikia N. Influence of curing conditions on the mechanical performance of concrete containing recycled plastic aggregate. Constr Build Mater 2012;36:196–204.
[7] Saikia N, de Brito J. Use of plastic waste as aggregate in cement mortar and concrete preparation: a review. Constr Build Mater 2012;34:385–401.
[8] Albano C, Camacho N, Hernández M, Matheus A, Gutiérrez A. Influence of content and particle size of waste pet bottles on concrete behavior at different w/c ratios. Waste Manage 2009;29:2707–16.
[9] Choi YW, Moon DJ, Chung JS, Cho SK. Effects of waste PET bottles aggregate on the properties of concrete. Cem Concr Res 2005;35:776–81.
[10] Ismail ZZ, Al-Hashmi EA. Use of waste plastic in concrete mixture as aggregate replacement. Waste Manage 2008;28:2041–7.
[11] Silva R, de Brito J, Saikia N. Influence of curing conditions on the durability-related performance of concrete made with selected plastic waste aggregates. Cement Concr Compos 2013;35:23–31.
[12] Frigione M. Recycling of PET bottles as fine aggregate in concrete. Waste Manage 2010;30:1101–6.
[13] Chidiac SE, Mihaljevic SN. Performance of dry cast concrete blocks containing waste glass powder or polyethylene aggregates. Cement Concr Compos 2011;33:855–63.
[14] ISO 834. Fire resistance tests. Elements of building construction. Genève: International Standards Organization (ISO); 1975.
[15] Schneider U. Concrete at high temperatures – a general review. Fire Saf J 1988;13:55–68.
[16] Khoury GA. Effect of fire on concrete and concrete structures. Prog Struct Mater Eng 2000;2:429–47.
[17] Arioz O. Effects of elevated temperatures on properties of concrete. Fire Saf J 2007;42:516–22.
[18] Eurocode 2: Design of concrete structures – Part 1–2: General rules – Structural fire design. Brussels: European Committee for Standardization (CEN); 2004.
[19] Saidum SV, Hadjisophocleous G, Craft S. Properties of materials at elevated temperatures (draft). CIB-W014 Fire Safety, WG2 – Fire Performance of Materials, 2012.
[20] Li M, Qian CX, Sun W. Mechanical properties of high-strength concrete after fire. Cem Concr Res 2004;34:1001–5.
[21] Husem M. The effects of high temperature on compressive and flexural strengths of ordinary and high-performance concrete. Fire Saf J 2006;41:155–63.
[22] Chen B, Liu J. Residual strength of hybrid-fiber-reinforced high-strength concrete after exposure to high temperatures. Cem Concr Res 2004;34:1065–9.
[23] Xiao J, Falkner H. On residual strength of high-performance concrete with and without polypropylene fibres at elevated temperatures. Fire Saf J 2006;41:115–21.
[24] Forrest JCM. An international review of the fire resistance of lightweight concrete. Int J Cem Compos Lightweight Concrete 1980;2:81–94.
[25] Tanyildizi H, Coskun A. The effect of high temperature on compressive strength and splitting tensile strength of structural lightweight concrete containing fly ash. Constr Build Mater 2008;22:2269–75.
[26] Tanaçan L, Ersoy HY, Arpacıoğlu U. Effect of high temperature and cooling conditions on aerated concrete properties. Constr Build Mater 2009;23:1240–8.
[27] Netinger I, Varevac D, Bjegovic D, Morić D. Effect of high temperature on properties of steel slag aggregate concrete. Fire Saf J 2013;59:1–7.
[28] Zadeh VZ, Bobko CP. Nanoscale mechanical properties of concrete containing blast furnace slag and fly ash before and after thermal damage. Cement Concr Compos 2013;37:215–21.
[29] Xu Y, Wong YL, Poon CS, Anson M. Impact of high temperature on PFA concrete. Cem Concr Res 2001;31:1065–73.
[30] Aydin S, Baradan B. Effect of pumice and fly ash incorporation on high temperature resistance of cement based mortars. Cem Concr Res 2007;37:988–95.
[31] Saad M, Abo-El-Eneini SA, Hanna GB, Kotkatat MF. Effect of temperature on physical and mechanical properties of concrete containing silica fume. Cem Concr Res 1996;26:669–75.
[32] Poon CS, Shui ZH, Lam L. Compressive behaviour of fiber reinforced high-performance concrete subjected to elevated temperature. Cem Concr Res 2004;34:2215–22.
[33] Cree D, Green M, Noumowe A. Residual strength of concrete containing recycled materials after exposure to fire: A review. Constr Build Mater 2013;45:208–23.
[34] Heikal M. Effect of temperature on the physico-mechanical and mineralogical properties of Homra pozzolanic cement pastes. Cem Concr Res 2000;30:1835–9.
[35] Ho CM, Tsai WT. Recycled concrete using crushed construction waste bricks subject to elevated temperatures. Adv Mater Res 2011;152–153:1–10.
[36] Zega CJ, Di Maio AA. Recycled concrete exposed to high temperatures. Mag Concr Res 2006;58:675–82.
[37] Vieira JPB, Correia JR, de Brito J. Post-fire residual mechanical properties of concrete made with recycled concrete coarse aggregates. Cem Concr Res 2011;41:533–41.
[38] Terro MJ. Properties of concrete made with recycled crushed glass at elevated temperatures. Build Environ 2006;41:633–9.
[39] Correia JR, Marques AM, Pereira CMC, de Brito J. Fire reaction properties of concrete made with recycled rubber aggregate. Fire Mater 2012;36:139–52.
[40] Marques AM, Correia JR, de Brito J. Post-fire residual mechanical properties of concrete made with recycled rubber aggregate. Fire Saf J 2013;58:49–57.
[41] EN 933-1 – Tests for geometrical properties of aggregates – Part 1: determination of particle size distribution–Sieving method, Brussels: European Committee for Standardization (CEN); 1997.
[42] EN 933-2 – Tests for geometrical properties of aggregates – Part 2: determination of particle size distribution – Test sieves, nominal size of apertures, Brussels: European Committee for Standardization (CEN); 1995.
[43] EN 1097-6 – Tests for mechanical and physical properties of aggregates – Part 6: determination of particle density and water absorption, Brussels: European Committee for Standardization (CEN); 2000.
[44] EN 1097-3 – Tests for mechanical and physical properties of aggregates – Part 3: determination of loose bulk density and voids, European Committee for Standardization (CEN), Brussels, 1998.
[45] LNEC E-237 – Aggregates: Los Angeles abrasion test (in Portuguese), Lisbon: National Laboratory of Civil Engineering (LNEC); 1970.
[46] EN 933-4 – Tests for geometrical properties of aggregates – Part 4: Determination of particle shape – shape index, Brussels: European Committee for Standardization (CEN); 2008.

[47] ISO 11357 – Plastics – Differential scanning calorimetry (DSC) – Part 1: General principles. Genève: International Standards Organization (ISO), 1997.
[48] J. Faury. Le béton. Paris: Dunod; Troisième Édition, 1958.
[49] EN 206-1 – Concrete – Part 1: Specification, performance, production and conformity, Brussels: European Committee for Standardization (CEN); 2000.
[50] EN 12350-2 – Testing fresh concrete – Part 2: Slump-test, European Brussels: Committee for Standardization (CEN); 2009.
[51] EN 12350-6 – Testing fresh concrete – Part 6: Density, Brussels: European Committee for Standardization (CEN); 2009.
[52] EN 1992-1-2 – Eurocode 1 – Actions on structures - Part 1. 2: General rules – Actions on structures exposed to fire, Brussels: European Committee for Standardization (CEN); 2002.
[53] Rilem TC. 129-MHT. Compressive strength for service and accident conditions. Mater Struct 1995;28:410–4.
[54] EN 12390-3 – Testing hardened concrete - Part 3: compressive strength of test specimens, Brussels: European Committee for Standardization (CEN); 2009.
[55] EN 12390-6 – Testing hardened concrete – Part 6: tensile splitting strength of test specimens, Brussels: European Committee for Standardization (CEN); 2009.
[56] LNEC E-397 – Concrete: calculation of modulus of elasticity in compression (in Portuguese), Lisbon: National Laboratory of Civil Engineering (LNEC); 1993.
[57] EN 12504-4 – Testing concrete – Part 4: Determination of ultrasonic pulse velocity, Brussels: European Committee for Standardization (CEN); 2004.
[58] EN 12504-2 – Testing concrete in structures – Part 2: Non-destructive testing – Determination of rebound number, Brussels: European Committee for Standardization (CEN); 2012.
[59] LNEC E394 – Concrete: determination of water absorption by immersion – Testing at atmospheric pressure (in Portuguese), Lisbon: National Laboratory of Civil Engineering (LNEC); 1993.
[60] ASCE, Structural Fire Protection, ASCE Manuals and Reports on Engineering Practice No. 78, 1992. p. 258.
[61] ACI 216-1.07, Code Requirements for Determining Fire Resistance of Concrete and Masonry Construction Assemblies, Report by Joint ACI/TMS Committee 216, 2007. p. 32.
[62] Bamonte P, Felicetti R. High-temperature behaviour of concrete in tension. Struct Eng Int 2013;22(4):493–9.
[63] Phan LT, Carino NJ. Review of mechanical properties of HSC at elevated temperature. J Mater Civ Eng 1992;10(1):58–64.
[64] Chang YF, Chen YH, Sheu MS, Yao GC. Residual stress–strain relationship for concrete after exposure to high temperatures. Cem Concr Res 2006;36(10):1999–2005.
[65] Savva A, Manita P, Sideris KK. Influence of elevated temperatures on the mechanical properties of blende cement concretes prepared with limestone and siliceous aggregates. Cement Concr Compos 2005;27(2):239–48.